

# Thioflavin T fluorescence anisotropy: An alternative technique for the study of amyloid aggregation

Raimon Sabaté \*, Sven J. Saupe

*Laboratoire de Génétique Moléculaire des Champignons, Institut de Biochimie et de Génétique Cellulaires, UMR 5095 CNRS/Université de Bordeaux 2, 1 rue Camille St. Saëns, 33077 Bordeaux Cedex, France*

Received 29 May 2007  
Available online 19 June 2007

## Abstract

The process of amyloid polymerisation raises keen interest in particular because of the biomedical impact of this process. A variety of analytical methods have been developed to monitor amyloid formation. Thioflavin T (ThT) is the most commonly used dye for detection of amyloid aggregation. Nevertheless, ThT fluorescence enhancement is strongly dependent of fibril morphology. In this study using the HET-s prion fibril model, we show that amyloid formation can be monitored by measuring ThT fluorescence anisotropy. Kinetic parameters obtained by this method are identical to those determined by CD spectrometry. We propose that ThT anisotropy represent an interesting, simple and alternative technique to analyze the amyloid formation process.  
© 2007 Elsevier Inc. All rights reserved.

**Keywords:** Thioflavin T; Anisotropy; Amyloid; Prion; Kinetic aggregation; Dye binding; Fibrillogenesis; *Podospora anserina*; Protein aggregation; Fibril polymerisation

Amyloid fibrils are  $\beta$ -sheet rich protein polymers responsible for a number of fatal human protein deposition diseases [1]. Thioflavin T (ThT) is the most commonly used dye to diagnose amyloid fibril formation, both *ex vivo* and *in vitro* [2,3]. In spite of this wide spread use, the exact mechanism underlying specific and rapid binding to amyloid fibrils remains largely unknown. Generally, ThT undergoes a strong increase in fluorescence quantum yield (around 480 nm, when excited at 450 nm) upon binding to amyloid fibrils [3]. However, fibril induced ThT-fluorescence varies greatly depending on the considered amyloid peptide and can be extremely modest for certain amyloid models [3–5]. The ThT molecule consists of a pair of benzothiazole and benzaminic rings freely rotating around a shared C–C bond [6]. ThT behaves as a rotor molecule; it is believed that the increase in quantum yield upon binding results from the inhibition of this free rotation of the rings. In free ThT, when the rotation is not hindered, excited ThT

molecules can undergo a torsional relaxation which effectively competes with the radiative transition [7]. It is thus possible that the enhancement of fluorescence emission depends dramatically of the capacity of a given amyloid fibril to hinder the ThT ring free rotation [4]. In addition, in all of ThT binding reaction to macromolecules, there is an alteration of the ThT global Brownian tumbling that can be detected by an increase in fluorescence anisotropy.

Reliable characterisation of the fibrillogenesis kinetics of amyloid proteins is of uppermost importance for instance to study the effect of inhibitor molecules of potential pharmacological importance or of familial disease-associated mutations [8]. Aggregation kinetics can be monitored by absorbance and scattering determinations [9,10], sedimentation assays, circular dichroism (CD) [11,12], dynamic and static light scattering [13], Congo Red binding [14], ThT binding [15,16], electron microscopy (EM), atomic forces microscopy (AFM) [17] or Trp/Tyr anisotropy [18,19]. All of these instrumental techniques suffer some associated technical limitations. For instance, absorbance and scattering depend on the fibril morphology (in a

\* Corresponding author. Fax: +33 5 56 99 90 67.  
E-mail address: [sabate@ibgc.cnrs.fr](mailto:sabate@ibgc.cnrs.fr) (R. Sabaté).

non-obvious way) [20], CD only determines soluble species and amyloid fibrils usually undergo rapid precipitation, Congo Red is not a specific dye and it is a kinetic inhibitor molecule [21], the quantum yield of ThT fluorescence depends dramatically of amyloid fibril type and there is a number of amyloid fibrils with a very modest and unappreciable ThT fluorescence [4]. Obviously, Trp/Tyr anisotropy can only be applied to peptides and proteins containing such residues.

In the present study, we used HET-s prion fibrils as a model of amyloid fibrils leading to a low ThT fluorescence enhancement and show that amyloid aggregation kinetic can conveniently be monitor by following the increase in ThT fluorescence anisotropy. We propose that ThT anisotropy represents an interesting, simple alternative method to follow amyloid formation.

## Materials and methods

**HET-s expression and purification.** HET-s(218–289) protein expressed as a C-terminal histidine-tagged construct in *Escherichia coli* was purified under denaturing conditions (50 mM Tris at pH 7.2, 300 mM NaCl, and 6 M GuHCl buffer) by affinity chromatography on Talon histidine-tag resin (ClonTech). Buffer was exchanged by gel filtration on Sephadex G-25 column (Amersham) for 175 mM acetic acid. The protein was conserved at 4 °C. For expression of HET-s(218–289), 2 l DYT medium were inoculated with an overnight culture of BL21(DE3) bearing the plasmid to be expressed at 37 °C. When an OD600 of 0.8–1.0 was reached, the bacteria were induced with 1 mM of isopropyl-1-thio- $\beta$ -D-galactopyranoside for 2 h at 37 °C, then the culture were centrifuged and the cell pellet were frozen at –20 °C [11].

**ThT anisotropy determination and ThT relative fluorescence.** ThT anisotropy measurements were recorded using a Perkin-Elmer LS50 fluorescence spectrometer with an excitation wavelength of 450 nm and emission at 480 nm. ThT and protein concentration of 10  $\mu$ M at pH 7 and 37 °C were used. The anisotropy values were calculated using the following equation:  $A = (I_{VV} - GI_{VH}) / (I_{VV} + 2GI_{VH})$ , where  $A$  is the anisotropy and  $G = I_{HV} / I_{HH}$ , and V and H in the subscript represent the vertical or the horizontal position of the excitation and the emission polarizers. For a rigid system the maximum anisotropy value is 0.4 whereas for a freely rotating small molecule the anisotropy values are considerably smaller [22]. ThT relative fluorescence has been determined with an excitation wavelength of 450 nm and emission range from 470 to 570 nm and the emission at 480 nm was recorded. ThT and protein concentration of 25 and 10  $\mu$ M, respectively, at pH 7 and 37 °C were used.

**CD spectroscopy determination.** CD spectra measured at a spectral resolution of 1  $\text{cm}^{-1}$ , and a scan rate of 15  $\text{nm min}^{-1}$  was collected from the wavelength range 200–250 nm at 37 °C using a Jasco 810 spectropolarimeter with a quartz cell of 0.1 cm path length. The transition from non-aggregated (random coil) to amyloid aggregated form (principally  $\beta$ -sheet) can be conveniently followed by circular dichroism. The CD spectra were recorded every 5 min after a simple cell inversion and the ratio of two wavelengths (217 and 210 nm) were recorded [4].

**Treatment and fitting of data.** HET-s(218–289) aggregation process may be studied as an autocatalytic reaction using the equation  $f = (\rho \{ \exp[(1 + \rho)kt] - 1 \}) / \{ 1 + \rho \exp[(1 + \rho)kt] \}$  under the boundary condition of  $t = 0$  and  $f = 0$ , where  $k = k_n a$  (when  $a$  is the protein concentration) and  $\rho$  represents the dimensionless value to describe the ratio of  $k_e$  to  $k$ . By non-linear regression of  $f$  against  $t$ , values of  $\rho$  and  $k$  can be easily obtained, and from them the rate constants,  $k_e$  (elongation constant) and  $k_n$  (nucleation constant). The extrapolation of the growth portion of the sigmoid curve to abscissa ( $f = 0$ ), and to the highest ordinate value of the fitted plot, afforded two values of time ( $t_0$  and  $t_1$ ), which correspond to the lag time and to the time at which the aggregation was almost complete.

The half-aggregation time ( $t_{1/2}$ ) is the time at which half of HET-s monomers were aggregated ( $f = 0.5$ ) [9].

**ThT fixation determination.** ThT-amyloid HET-s(218–289) fixation was determined according to a centrifugation method. ThT at 25  $\mu$ M was mixed with a range from 0 to 20  $\mu$ M of protein for 30 min. In order to precipitate the ThT–HET complex a centrifugation at 10,000g for 30 min was used. ThT absorbance at 411 nm ( $\lambda_{\text{max}}$ ) was recorded at 37 °C before and after centrifugation using a Perkin-Elmer Lambda Bio 20 UV/vis spectrophotometer using a matched pair of quartz cuvettes of cm optical length placed in a thermostated cell holder, at 37 °C [23].

**Electron microscopy.** For negative staining, samples were adsorbed to freshly glow-discharged carbon-coated grids, rinsed with water, and stained with 1% uranyl acetate. Samples of pH 7 fibrils were usually sonicated shortly (5 s on a Kontes sonicator at about 60 W) to assure optimal particle size. Micrographs were recorded on a Philips CM120 microscope.

## Results and discussion

The HET-s(218–289) fungal prion protein undergoes a spontaneous transition from a random coil to a  $\beta$ -sheet rich structure at pH 7 in 1:1 mixture of 175 mM acetic acid and 1 M Tris pH 7.2 (high ionic strength) [24]. In this buffer, ordered bundles of laterally-associated fibrils are detected by EM (Fig. 1A). The elementary fibrils are  $\sim 5$  nm in

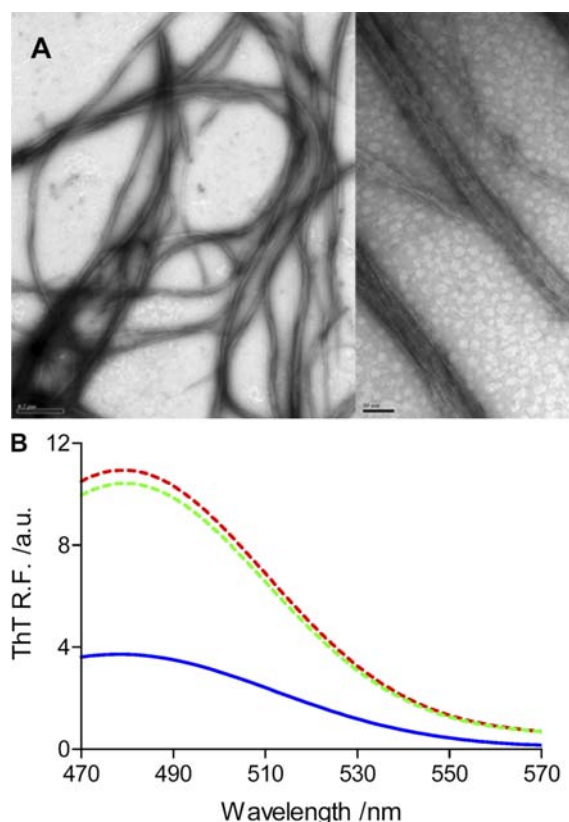


Fig. 1. Electron micrographs and ThT fluorescence of pH 7 HET-s(218–289) fibrils. (A) Electron micrographs showing amyloids formed at pH 7 at 37 °C in high ionic strength consisting of ordered bundles containing variable number of 5 nm fibrils. (B) ThT fluorescence without (blue continuous line) and with 10  $\mu$ M of HET-s in random coil form (green dotted line) and assembled pH 7 fibrils (red continuous line). (For interpretation of the references to colour in this figure legend, the reader is referred to the web version of this article.)

diameter. The bundles are highly variable in width and may exceed 100–200 nm representing an important stack of fibrils [4]. The ThT fluorescence for fibrils assembled at pH 7 is extremely modest and the difference of ThT spectra between random coil and amyloid form is practically unappreciable (Fig. 1B). Nonetheless, ThT is bound to the fibrils in this condition. Indeed, when we applied a centrifugation method to estimate the amount of fibril bound ThT, we obtained a fixation from 1.1 to 1.7  $\mu\text{M}$  of ThT when 25  $\mu\text{M}$  of ThT are mixed with a range from 5 to 20  $\mu\text{M}$  of protein in fibrillar form. ThT fixation without associated quantum yield enhancement could be explained by a partial fixation of the ThT molecule. Possibly, this interaction is insufficient to block the rotation of the rings and thus ensure quantum yield enhancement. Alternatively, it might be that the geometry of the bound ThT dictated by the fibril twist is unfavourable to the quantum yield enhancement. Nevertheless, since ThT is fibril bound we reasoned that the dye molecule should display a marked increase in fluorescence anisotropy due to reduction of Brownian tumbling.

In aqueous solutions, ThT was found to exist as micelles at concentrations commonly used to monitor fibrils by fluorescence assay ( $\sim 10$ – $20 \mu\text{M}$ ) [22]. We have determined that micellar association does not affect the quantum yield of fluorescence of ThT (Supplementary 1A) but it increases dramatically the motion of ThT molecule in micellar form. This latter physical–chemical property allows determining the critical micellar concentration (cmc) of ThT molecule. In our study conditions, a value of 13.7  $\mu\text{M}$  has been obtained (Supplementary 1B). In order to avoid the micelle effect in the ThT mobility, the ThT concentration used in kinetic aggregation essays was kept below the cmc value.

As can be observed in Fig. 2A, ThT anisotropy allows monitoring of the HET-s aggregation kinetic. The ThT anisotropy value can be easily transformed into aggregated fibril fraction that allows determining the nucleation ( $k_n$ ) and elongation ( $k_e$ ) constants (Fig. 2C) of the nucleation–polymerisation process that underlies amyloid formation. In order to estimate the reliability of the ThT anisotropy method, the aggregation process was also analyzed by CD spectroscopy. A combination of hydrogen exchange, solid state NMR and proline-scanning mutagenesis data has led to a model for the infectious amyloid fold of HET-s(218–289) [25]. It comprises four  $\beta$ -strands forming a  $\beta$ -roll structure [25]. Recent evidence further supports this  $\beta$ -roll model. HET-s(218–289) fibrillization is thus accompanied by a marked increase in  $\beta$ -sheet content. HET-s(218–289) amyloid polymerisation was followed by CD spectroscopy by detecting the transition from a random-coil structure to a principally  $\beta$ -sheet structure (amyloid form) [26]. As can be observed in Fig. 2B and Fig. 2C, the kinetic measured by ThT anisotropy and CD spectroscopy are nearly identical. HET-s aggregation kinetic has been assimilated to an autocatalytic reaction. A mathematical analysis allows determining the rates constants and the

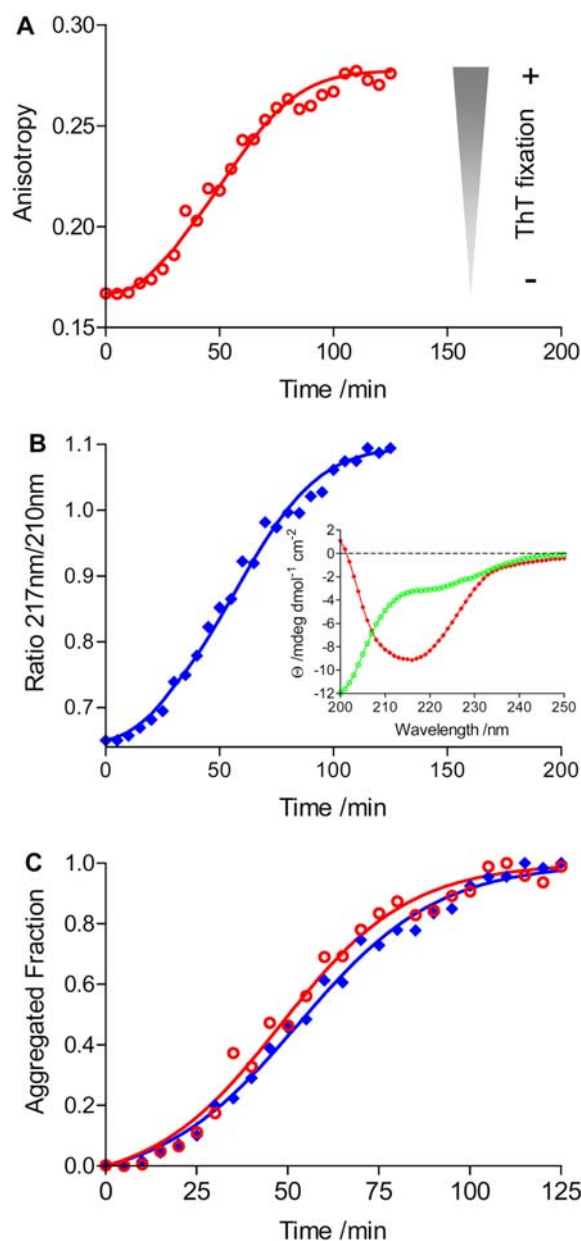


Fig. 2. Kinetic of aggregation of 10  $\mu\text{M}$  of HET-s(218–289) at pH 7 and 37 °C. (A) Kinetic of aggregation monitored by ThT anisotropy. (B) CD spectroscopy, inset, CD spectra of random coil (○) and fibril (◆). (C) Experimental (○) and fitted (red line) ThT anisotropy, and experimental (◆) and fitted (blue line) CD spectroscopy values transformed into fraction of aggregated form. (For interpretation of the references to colour in this figure legend, the reader is referred to the web version of this article.)

times of reaction obtaining  $k_n$ ,  $k_e$ , lag time ( $t_0$ ), half-time ( $t_{1/2}$ ), and complete reaction time ( $t_1$ ) values [9]. Comparing the kinetic values obtained by CD spectroscopy and ThT anisotropy presented in Table 1., it is clear that both analytical techniques lead to very similar kinetic constants and times. These results confirm that ThT anisotropy can be an excellent and alternative analytic method to study the amyloid aggregation kinetic and amyloid fibril formation.

In order to compare results obtained by ThT anisotropy and Trp/Tyr anisotropy, we analyzed Trp/Tyr anisotropy



Table 1  
Aggregation kinetic parameters

	ThT anisotropy	CD spectroscopy
$k_n/\text{mol}^{-1} \text{ dm}^3 \text{ min}^{-1}$	5305	4872
$k_d/\text{min}^{-1}$	0.0035	0.0031
$t_0/\text{min}$	15	16
$t_{1/2}/\text{min}$	50	55
$t_1/\text{min}$	85	93

in the random coil and fibrillar form. Using Trp/Tyr anisotropy, we have obtained a value of  $0.069 \pm 0.012$  and  $0.095 \pm 0.013$  for random coil and fibril form, respectively. This minimal Trp/Tyr anisotropy variation makes it impossible to monitor HET-s aggregation by this method. A possible explanation at this very poor Trp/Tyr anisotropy difference could be relate to the fact that in the random coil state, HET-s(218–289) forms random coil oligomeric structures rather than isolated monomers (R.S., unpublished results), a situation previously reported for the Sup35 yeast prion protein [27].

Measuring amyloid formation is usually difficult. The fibrillogenesis process can lead to protein precipitation, aggregate transformation and fibril morphology alterations that can affect various analytical techniques used to analyze this aggregation process. ThT is considered a specific amyloid detector, however ThT quantum yield enhancement is very dependent to amyloid morphology and not all amyloid fibrils induce a measurable ThT fluorescence enhancement. ThT anisotropy allows determining the ThT fixation independently of ThT fluorescence enhancement making this analytical technique in a new and useful system to monitor the aggregation process especially when amyloid fibrils fix the ThT molecule without inducing a dramatic fluorescence enhancement.

## Appendix A. Supplementary data

Supplementary data associated with this article can be found, in the online version, at [doi:10.1016/j.bbrc.2007.06.063](https://doi.org/10.1016/j.bbrc.2007.06.063).

## References

- [1] F. Chiti, C.M. Dobson, Protein misfolding, functional amyloid, and human disease, *Annu. Rev. Biochem.* 75 (2006) 333–366.
- [2] H. Naiki, K. Higuchi, M. Hosokawa, T. Takeda, Fluorometric determination of amyloid fibrils in vitro using the fluorescent dye, Thioflavin T1, *Anal. Biochem.* 177 (1989) 244–249.
- [3] H. LeVine, Quantification of  $\beta$ -sheet amyloid fibril structures with Thioflavin T, *Methods Enzymol.* 309 (1999) 274–284.
- [4] R. Sabaté, U. Baxa, L. Benkemoun, N. Sánchez de Groot, B. Couлары-Salin, M.L. Maddelein, L. Malato, S. Ventura, A.C. Steven, S.J. Saupe, Prion and non-prion amyloids of the HET-s prion forming domain, *J. Mol. Biol.* (2007), doi:10.1016/j.jmb.2007.05.014.
- [5] K. Murakami, K. Irie, A. Morimoto, H. Ohigashi, M. Shindo, M. Nagao, T. Shimizu, T. Shirasawa, Neurotoxicity and physicochemical properties of A $\beta$  mutant peptides from cerebral amyloid angiopathy: implication for the pathogenesis of cerebral amyloid angiopathy and Alzheimer's disease, *J. Biol. Chem.* 278 (2003) 46179–46187.
- [6] W. Dzwolak, M. Pecul, Chiral bias of amyloid fibrils revealed by the twisted conformation of Thioflavin T: an induced circular dichroism/DFT study, *FEBS Lett.* 579 (2005) 6601–6603.
- [7] V.I. Stsiapura, A.A. Maskevich, V.A. Kusmitsky, K.K. Turoverov, I.M. Kuznetsova, Computational study of thioflavin T torsional relaxation in the excited state, *J. Phys. Chem. A* (2007), doi:10.1021/jp070590o.
- [8] R. Sabaté, J. Estelrich, Stimulatory and inhibitory effects of alkyl bromide surfactants on beta-amyloid fibrillogenesis, *Langmuir* 21 (2005) 6944–6949.
- [9] R. Sabaté, M. Gallardo, J. Estelrich, An autocatalytic reaction as a model for the kinetics of the aggregation of beta-amyloid, *Biopolymers* 71 (2003) 190–195.
- [10] K.C. Evans, E. Berger, C. Cho, K.H. Weisgraber, Apolipoprotein E is a kinetic but not thermodynamic inhibitor of amyloid formation: implications for the pathogenesis and treatment of Alzheimer disease, *Proc. Natl. Acad. Sci. USA* 92 (1995) 763–767.
- [11] L. Benkemoun, R. Sabate, L. Malato, S. Dos Reis, H. Dalstra, S.J. Saupe, M.L. Maddelein, Methods for the in vivo and in vitro analysis of [HET-s] prion infectivity, *Methods* 39 (2006) 61–67.
- [12] C. Goldsbury, K. Goldie, J. Pellaud, J. Seelig, P. Frey, S.A. Müller, J. Kistler, G.J.S. Cooper, U. Aebi, Amyloid fibril formation from full-length and fragments of amylin, *J. Struct. Biol.* 130 (2000) 352–362.
- [13] A. Lomakin, D.S. Chung, G.B. Benedek, D.A. Kirschner, On the nucleation and growth of amyloid  $\beta$ -protein fibrils: detection of nuclei and quantitation of rate constants, *Proc. Natl. Acad. Sci. USA* 93 (1996) 1125–1129.
- [14] R.M. Murphy, Peptide aggregation in neurodegenerative disease, *Annu. Rev. Biomed. Eng.* 4 (2002) 155–174.
- [15] H. Naiki, F. Gejyo, Kinetic analysis of amyloid fibril formation, *Methods Enzymol.* 309 (1999) 305–318.
- [16] B. O'Nuallain, S. Shivaprasad, I. Kheterpal, R. Wetzel, Thermodynamics of A $\beta$ (1–40) amyloid fibril elongation, *Biochemistry* 44 (2005) 12709–12718.
- [17] C. Goldsbury, J. Kistler, U. Aebi, T. Arvinte, G.J.S. Cooper, Watching amyloid fibrils grow by time-lapse atomic force microscopy, *J. Mol. Biol.* 285 (1999) 33–39.
- [18] B.W. Koo, A.D. Miranker, Contribution of the intrinsic disulfide to the assembly mechanism of islet amyloid, *Protein Sci.* 14 (2005) 231–239.
- [19] P.O. Souillac, V.N. Uversky, A.L. Fink, Structural transformations of oligomeric intermediates in the fibrillation of the immunoglobulin light chain LEN, *Biochemistry* 42 (2003) 8094–8104.
- [20] J.D. Harper, P.T. Lansbury, Models of amyloid seeding in Alzheimer's disease and scrapie, *Annu. Rev. Biochem.* 66 (1997) 385–407.
- [21] R. Khurana, V.N. Uversky, L. Nielsen, A.L. Fink, Is Congo Red an amyloid-specific dye? *J. Biol. Chem.* 276 (2001) 22715–22721.
- [22] R. Khurana, C. Coleman, C. Ioanescu-Zanetti, S.A. Carter, V. Krishna, R.K. Grover, R. Roy, S. Singh, Mechanism of thioflavin T binding to amyloid fibrils, *J. Struct. Biol.* 151 (2005) 229–238.
- [23] R. Sabaté, J. Estelrich, Pinacyanol as effective probe of fibrillar  $\beta$ -amyloid peptide: Comparative study with Congo Red, *Biopolymers* 72 (2003) 455–463.
- [24] A. Baluegier, S. Dos Reis, C. Ritter, S. Chaignepain, B. Couлары-Salin, V. Forge, K. Bathany, I. Lascu, J.M. Schmitter, R. Riek, S.J. Saupe, Domain organization and structure-function relationship of the HET-s prion protein of *Podospora anserine*, *EMBO J.* 22 (2003) 2071–2081.
- [25] C. Ritter, M.L. Maddelein, A.B. Siemer, T. Luhrs, M. Ernst, B.H. Meier, S.J. Saupe, R. Riek, Correlation of structural elements and infectivity of the HET-s prion, *Nature* 435 (2005) 844–848.
- [26] A. Sen, U. Baxa, M.N. Simon, J.S. Wall, R. Sabate, S.J. Saupe, A.C. Steven, Mass analysis by scanning transmission electron microscopy and electron diffraction validate predictions of the stacked beta-solenoid model of HET-s prion fibrils, *J. Biol. Chem.* 282 (2007) 5545–5550.
- [27] T. Serio, A. Cashikar, A. Kowal, G. Sawicki, J. Moslehi, L. Serpell, M. Arnsdorf, S. Lindquist, Nucleated conformational conversion and the replication of conformational information by a prion determinant, *Science* 289 (2000) 1317–1321.